Evaluate the variation of (Ver. 1 & 3) ASTER Global DEM Datasets for the Sanam Mountain – Iraq

Amal Jabbar Hatem [1, a)], Hameed M. Abduljabbar [1, b)], Taghreed Abdulhameed Naji [1, c),] and Shahad Abdul Qader Abdul Hameed [2, d)]

[1]*Department of Physics, College of Education for pure science, Ibn-Al-Haitham, University of Baghdad, Baghdad, Iraq 10001*
[2]*Ministry of Water Resources, Baghdad, Iraq 10001*

[a)] amal.j.h@ihcoedu.uobaghdad.edu.iq
[b)] hameed.m.aj@alKutcollege.edu.iq
[c)] taghreed.ah.n@ihcoedu.uobaghdad.edu.iq
[d)] *Corresponding author* Shahed.Abd1204a@ihcoedu.uobaghdad.edu.iq

ABSTRACT. The most important geomorphological systems are determining elevations and contour maps of land features. In this research, two satellite scene versions of ASTER GDEM (1 and 3) were utilized to examine the relief and geomorphological statistics of Sanam Mountain in Basra Province. The study, through a comparison of the shading shapes of Sanam Mountain for both ASTER GDEM versions and the Sentinel-2 satellite image, showed that the surface relief of the ASTER GDEM Ver. 1 is closer to the real scene of the mountain. In contrast, the boundary and recorded elevation for the highest peak were better represented by Ver. 3., which was closer to the real elevation of field measurements. **KEYWORDS.** Digital Elevation Model, Stereoscopic vision, Geomorphological analysis, ASTER GDEM Spaceborne.

INTRODUCTION

Elevation data, contours, and maps for a certain region can be represented as a 3D model using a digital elevation model (DEM), where it plays a significant role in reconstructing landform and elevation accuracy of the earth sciences and the regional geomorphology research. When other sources of data regarding the height of the study site are absent, it serves as the only source of information [1,2,3,4]. Currently, there are numerous freely accessible worldwide DEMs, including (GLOBE DEM, SRTM, GTOPO 30, ASTER DEM, AW3D30, DTED-2, EU-DEM). Their spatial resolution ranges from 30 m to 1 km. The kind and degree of relief, the techniques used to collect elevation data, DEM generation, and DEM spatial resolution are only a few of the variables that affect how accurate a DEM is. The quality of the DEM created from topographic map data is crucial for determining the validity of geomorphometric analysis [5,6,7,8,9]. Global Digital Elevation Model (GDEM) of the Earth's land surface was jointly issued by the National Aeronautics and Space Administration (NASA) of the United States and Japan's Ministry of Economy, Trade, and Industry (METI), to validate and characterize its model that derived from the optical stereo data acquired by the Advanced Spaceborne Thermal Emission and Reflection Radiometer (ASTER) satellite, through the Earth Remote Sensing Data Analysis Center (ERSDAC) and the NASA Land Processes Distributed Active Archive Center (LP DAAC) at no charge to users worldwide as an assistance to the Global Earth Observing System of Systems (GEOSS). ASTER GDEM was released in Version 1 on 29 June 2009, as a publicly available DEM. It was the first freely available DEMs on a global scale, the sole DEM with high resolution coverage of the whole Earth's land surface, it has greatly contributed to the global earth observing community and has been widely used by many users. This high-resolution global DEM product was developed based on data from the optical sensors ASTER by collecting along-track stereoscopic capability over the terrain. Two NIR cameras on the ASTER satellite were used to produce the GDEM. One faces the nadir while the other is tilted in the direction of the along-track. The images produce overlapping stereo imagery after a brief delay, enabling the creation of a photogrammetric DEM [10,11,12,13]. The ASTER GDEM Ver.1 methodology utilized automated processing for the whole ASTER archive, using (1,264,118) individual scenes by the stereo correlation. It was produced by stacking all individual cloud-masked scene DEMs and non-cloud-masked image DEMs as reference data, and then using different methods (statistical approach) to repair and replace abnormalities or missing data into (1° × 1°) tiles [14,15,16,17]. Stereoscopic vision can be defined as the ability to

classify features in the 3D world to estimate depth. The acquired stereo data was photogrammetrically processed for satellite (ASTER GDEM Ver.1 stereo images) triangulation using the rational polynomial coefficients (RPCs) to generate DEM. Photogrammetry is applied for mapping using very high-resolution stereoscopic satellite images [18,19,20]. In August 2019, the ASTER Science Team released the final version of the GDEM, GDEM3, by the Land Processes Distributed Active Archive Center (LP DAAC), which provides global spatial coverage. Several hundred thousand additional scenes were added to produce data of the highest quality and with the strictest automatic and manual anomaly correction program GDEM possible, where the ASTER GDEM Ver. 3 images have cloud coverage because ASTER is an optical sensor. It provided a global digital elevation model (DEM) of land areas on Earth at a spatial resolution of 1 arc-second (30 m) posting horizontally at the equator. The National Aeronautics and Space Administration (NASA) and Japan's Ministry of Economy, Trade, and Industry (METI) collaborated to create the ASTER GDEM data versions. The Tokyo-based Sensor Information Laboratory Corporation (SILC) creates the ASTER GDEM data versions. [14,21].

A literature review for related work is:

Guosong Zhao and et.al., 2010 [22] studied the performance of the Global Digital Elevation Model (GDEM) from optical stereo data acquired by ASTER GDEM v1 and SRTM (the Shuttle Radar Topography Mission) satellites. They showed the better performance of ASTER GDEM v1 in the flat regions than in the mountainous regions, due to its having many anomalies in data, which are caused by the methodology to produce the ASTER GDEM v1, it had lower elevations approximately (5 m) compared with the SRTM. They recommended should improve the DEM quality of the ASTER GDEM and a filter operation was used to remove the anomalies data.

K. Jacobsen and R. Passin, 2010 [23] analyzed and compared the ASTER GDEM with SRTM DEM, SPOT 5 HRS, and Cartosat 1 height models. They showed that the ASTER GDEM in most conditions had an improved accuracy with a higher number of images used for overlapping height models, depending upon the region, especially in regions with low cloud coverage. They illustrated that the ASTER and SRTM height models are dependent upon the morphology and the land cover, so no homogeneous accuracy can be predicted, where the accuracy for these height models depends usually linearly upon the tangent of terrain slope, not only the standard deviation, the height models have different regular errors.

Bernadett Dobre and et.al, 2021 [24] illustrated the limitations and advantages of the digital elevation models (DEMs) covering the Desatoya study region, (such as TDX-12, LIDAR30, SRTM1, ASTER GDEM, AW3D30, TDX-30, SRTM3, TDX-90, and MERIT), which is created from different acquisition methods and at various spatial resolutions, through extracting geomorphic surface remnants in a semi-arid, mountainous topographic environment. They confirmed that although the tested models were known, their accuracy of peak detection is needed for the study. They determined the peaks as remnants of degraded geomorphic surfaces from both a statistical and a geomorphometric approach, which can help to reconstruct geomorphic surfaces, availability of information on the previous erosion processes, and the present state of the surfaces, and evaluate DEM applicability to set the overall accuracy and paleo surface detection.

The main goal of this research is to study the validity of the first and third versions of ASTER GDEM that released in 2009 & 2019 respectively to describe the relief digital elevations by comparing the shape and its statistics and the highest elevation (peak value) for the study area at (Sanam mountain), which located in Basra province, Iraq.

METHOD AND MATERIAL

Study region description and the data used

The study location is in the Al-Zubair area of Basra province, which is in southern Iraq. Figure 1 shows the geographic location of the available data, as illustrated in Table 1, with different sensors, and a geological map for southern Iraq (Determined the study region by a red frame (see Figure 1 (D & E)). The satellite scenes were downloaded from ERSDAC and NASA's Land Processes Distributed Active Archive Center (LP DAAC), and the United States Center for Earth Resources, Observation, and Science [25,26,27,28].

Table (1). Information about the satellite scenes used

Satellite	Spatial Resolution	Site Location	Released Date	Scene Dimensions (pixels)
ASTER GDEM Ver.1	1 arc-second (30 m)	N30 and E47	29 June 2009	3600 × 3600
ASTER GDEM Ver.3	1 arc-second (30 m)	N30 and E47	August 2019	3600 × 3600
Sentinel-2	20 m	Path 166 / Row 039	25 July 2019	10980 × 10980

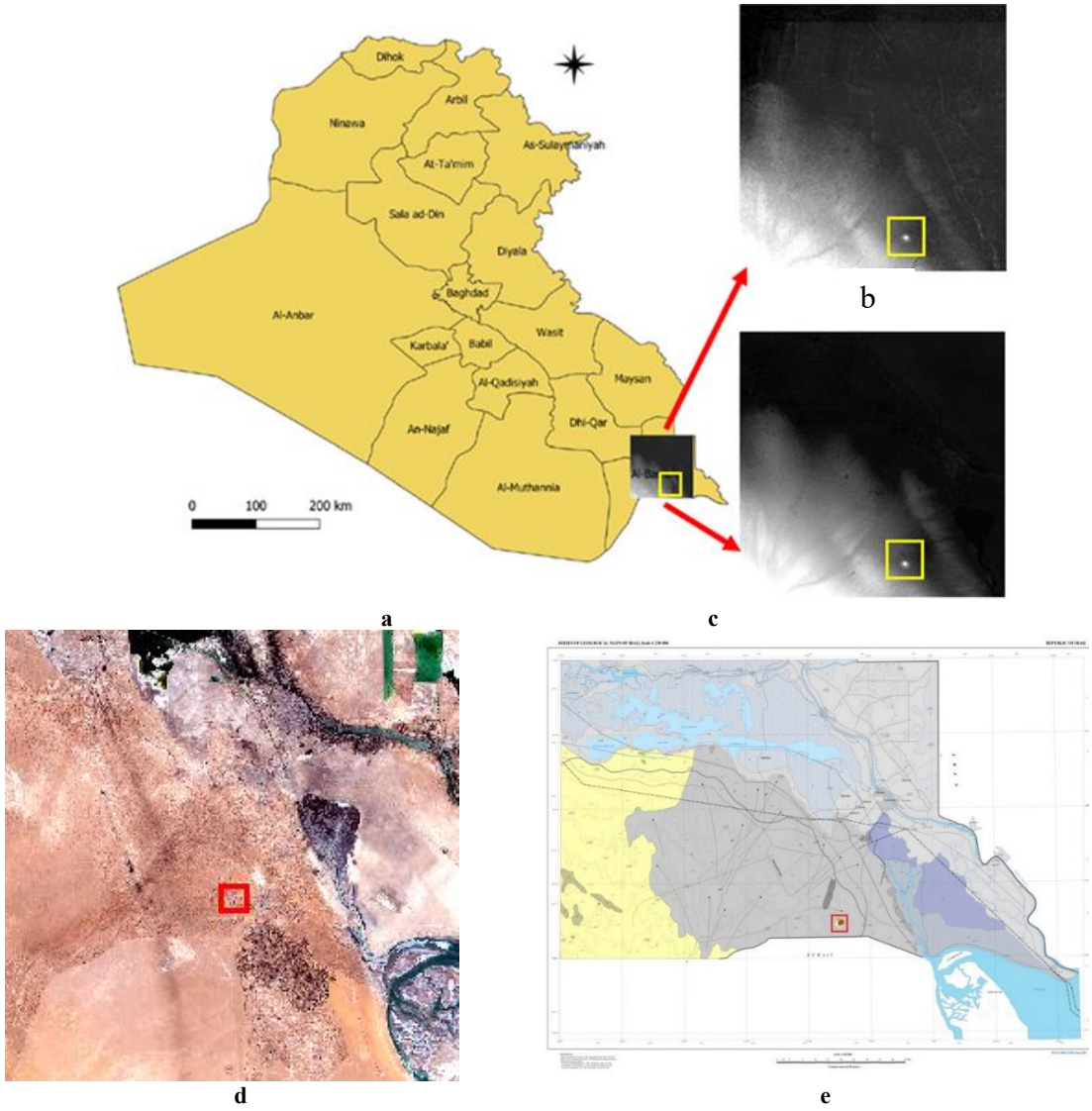

FIGURE 1. ASTER scenes on; (a) Iraq map, of (b) ASTER GDEM Ver.1, (c) ASTER GDEM Ver.3, d & e) the true color of Sentinel-2 scene, and a geological map for southern Iraq [29]

In this research, the Sanam Mountain was chosen as a study region. This mountain constitutes the prominent geomorphic attributes in the southwest of Iraq, and it lies about 48 km south of Basra province [30]. This Sanam Mountain lies in the Dibdiba plain, which belongs to the Mesopotamian Zone, and it has an unstable shelf. On the other hand, concerning the tectonic divisions of Iraq. This structure can be found inside the basins of the region between the river valleys that constitute the Arabian plate's folds. [31,32,33,34,35]. The term mountain is used for public naming, it is not a mountain because its elevation is less than the mountain height (600 m) above sea level, being the only hill elevated and isolated in the city of Basra province, as defined by Fairbridge [32].

RESEARCH METHODOLOGICAL

The process that has been made can be described through this summary:

1. Determine the threshold value that separates the Sanam Mountain from the adjacent regions.
2. Isolate the Sanam Mountain.
3. Calculate the mountain geomorphological factors and statistics.
4. Constructing the mountain shading shape for both ASTER GDEM versions.

5. Comparing the two shading shapes with a real image of the mountain captured by the Sentinel-2 satellite image on 25 July 2019, and the highest elevation of the two DEMs with a field data measurement.

RESULTS AND DISCUSSIONS

Determining the boundaries of the mountain is an important point in this research, so that we can judge the validity of the digital elevation model for the two versions of the ASTER GDEM, using the QGIS 3.26 program, to study the digital elevation models for the two versions based on the change in elevation around the mountain. The height of 30 m above sea level was chosen as the starting point, the boundaries of the mountain, because the average height of the land around the mountain ranges from (27-29) m above sea level. When it rises 30 m above sea level, the altitude begins to increase rapidly to form Sennam Mountain. The region above 30 m was chosen to be the outer boundary of the mountain, as shown in Figure 2, on which the contour lines are shown to distribute the heights of the mountain with an interval of 10 m between one line and another.

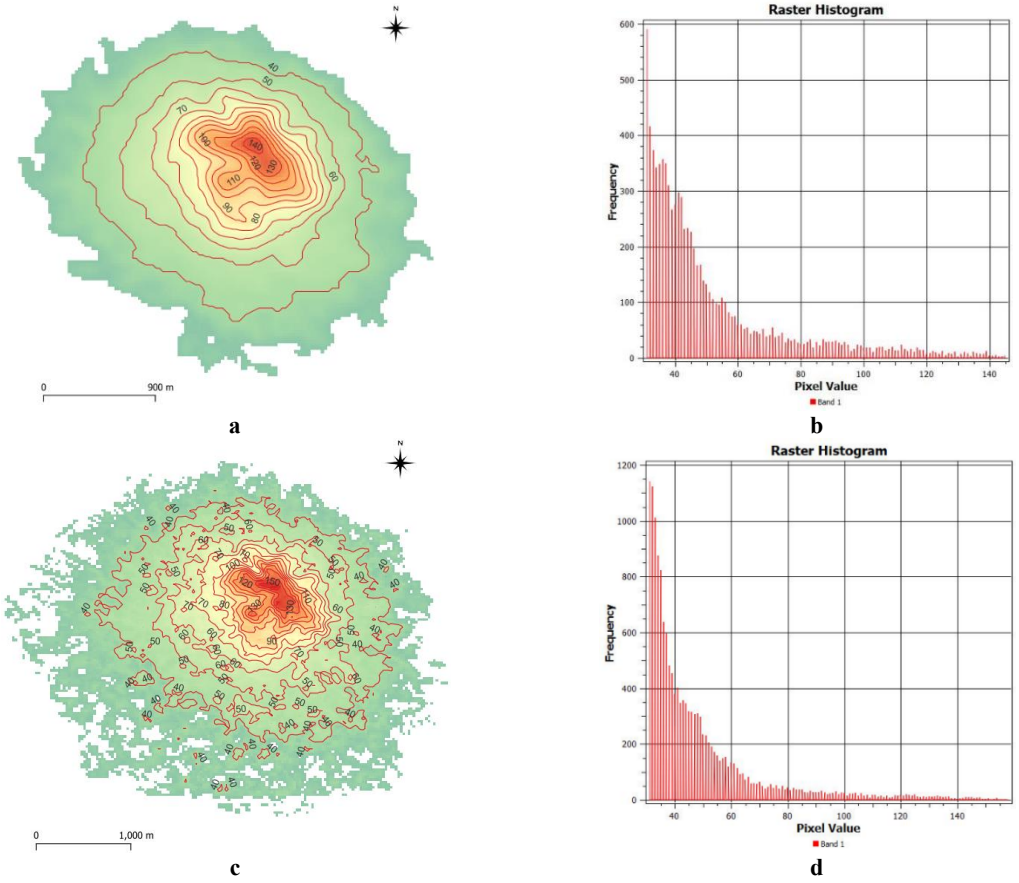

FIGURE 2. The elevation contours with 10 m interval value for; (a) ASTER GDEM Ver. 1, (b) its histogram, (c) ASTER GDEM Ver. 3, and (d) its histogram

It can be seen that the diversity of elevations in the ver. 1 is much more than in the ver. 3 as shown in the probability distribution function (histogram) curve of the digital elevation models, although the Sanam mountain relief in the ver. 1 is less than the ver. 3. The Geomorphological statistics characteristics, such as (minimum, maximum, mean, and standard deviation elevation, area, and volume) of the mountain were calculated for both digital elevation models, as shown in Table 2.

Table (2). Geomorphological statistics of Sanam Mountain for the two ASTER GDEM versions

Satellite	Min Elevation	Max Elevation	Mean Elevation	STD Elevation	Area m^2	Volume m^3

ASTER GDEM Ver.1	31	145	51.06071	22.99353	7605000	388316736
ASTER GDEM Ver.3	31	158	47.7677718	21.1553326	13382100	639233024

According to figure 3 and table 1, the locations of Sanam mountain using ASTER GDEM Ver.1, and Ver.3 are specified between (30° 8' 17.01"- 30° 6' 25.01") latitude and (47° 36' 16.00" - 47° 38' 27.01") longitude with an area of about (760.5 *k*m2), and (30° 8' 26.51"- 30° 6' 6.51") latitude and (47° 35' 71.51" - 47° 38' 39.51") longitude with an area of about (1338.21 *k*m2), respectively. The Sanam mountain shading shapes of both ASTER GDIM versions are constructed to find the best matching for these images, by comparing them with the mountain shape using the Sentinel-2 satellite image, which overlays the boundary of the Ver1 (blue line) and Ver3 (red line) mountain DEM, as shown in Figure 3.

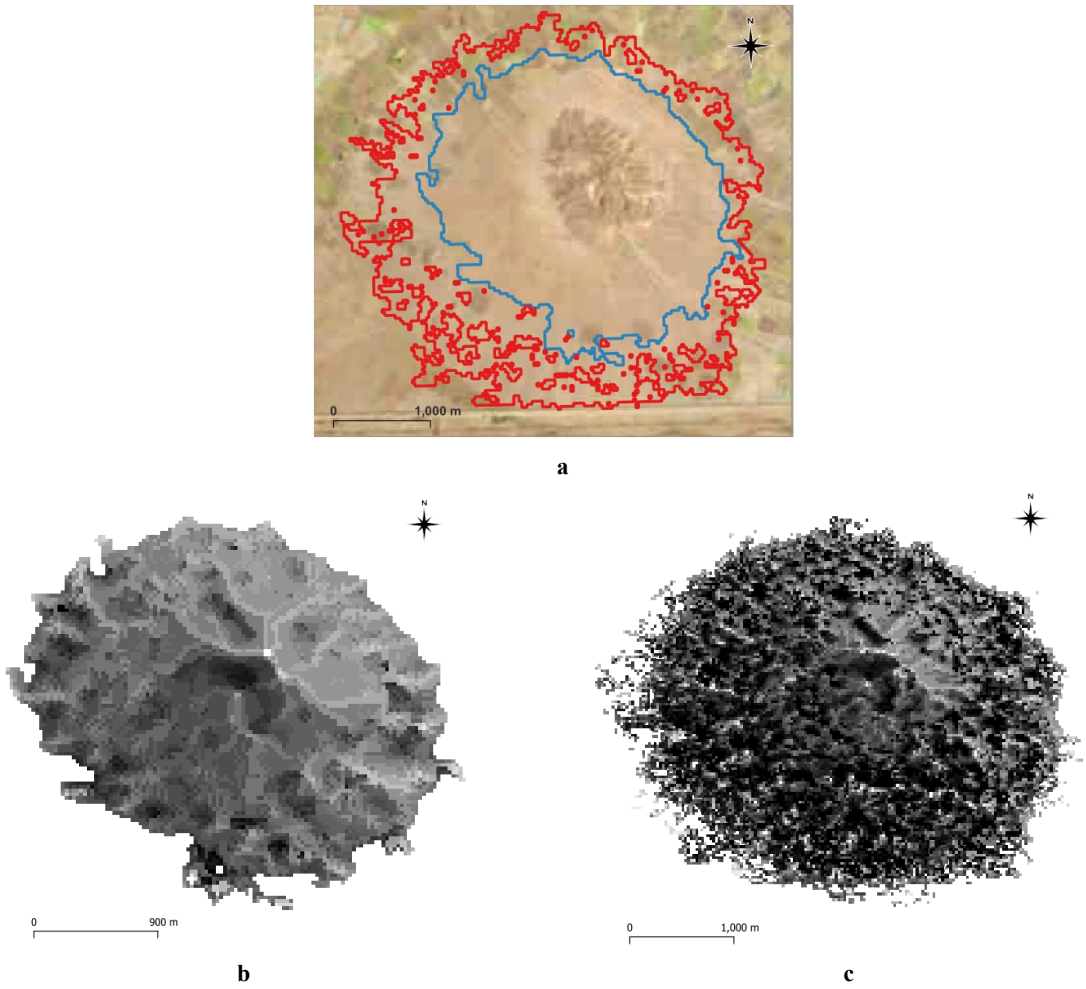

FIGURE 3. (a) Sentinel-2 image, (b) shading shapes of ASTER GDEM ver.1, and (c) ver.3

By comparing the mountain boundary for ver.1 (blue line) and the Sentinel-2 satellite image in (figure 3a), it was less than the real boundaries, while the ver. 3 was closer to the optimal border of the mountain (red line), which leads to the mountain base area and volume being less than the right value for ver. 1, in contrast to ver. 3, since the area and the volume are closer to the right value. One more thing can be noticed by comparing the mountain surface relief of the two GDEM versions with the Sentinel-2 satellite image, in the ver. 1, The surface relief of the mountain is closer to the surface relief in the satellite image. Unlike the ver. 3, where the shape of the surface relief is much coarse to the surface relief of the mountain in a satellite image, given that the spatial resolution of the mountain taken by the Sentinel-2 satellite is (20 m), unlike the spatial resolution of the ASTER GDEM which is (30 m), i.e. the surface

relief of the mountain in the shading shape of the two ASTER GDEM versions is less than what it is in a satellite image. As for the elevation of the highest peak in the mountain, it was recorded for the ver. 3 closer to the real elevation of the mountain, which was measured in the field, where the difference in the elevation measurement for the ver. 3 is (1 m), and for the ver. 1 is (12 m). As for the location of the highest peak in the mountain, it was determined correctly and identical to both versions, compared to the field measurement of the highest peak, as shown in Table 3.

Table (3). Mountain's highest elevation and its location for ASTER GDE two versions, with field measurement

Satellite ASTER	Max. Elevation	Latitude coordinate	Longitude coordinate	Real Elevation	Real Latitude	Real Longitude	Elevation Difference	Latitude Difference	Longitude Difference
Ver.1	145	30⁰ 07´ 37"	47⁰ 37´ 29"	157	30⁰ 07´ 33"	47⁰ 37´ 24"	-12	+4"	+5"
Ver.3	158	30⁰ 07´ 37"	47⁰ 37´ 30"				+1	+4"	+6"

CONCLUSIONS

The third version of the ASTER GDEM was able to determine the boundary and the highest peak of Sanam Mountain in a manner that is close to reality, unlike the first version, which failed in this regard. Sanam Mountain, through the first version, is closer to the surface relief found in Sanam Mountain. Accordingly, we find that the last (third version) of the ASTER GDEM is better for studying the structural forms of the Earth's surface, keeping in mind that the shape of the recorded surface relief of this version is an exaggeration of what exists.

REFERENCES

1. H I Reuter, T Hengl, P Gessler, and P Soille, "Preparation of DEMs for Geomorphometric Analysis," Geomorphometry: Concepts, Software, Applications. Developments in Soil Science, 33, (1), pp. 87–120, 2009. DOI:10.1016/S0166-248100004-4.
2. Israa Jameel Muhsin, "High spatial resolution digital elevation model (DEM) production using different interpolations techniques," Iraqi Journal of Physics, 11(21), pp. 116-126, 2013. https://doi.org/10.30723/ijp.v11i21.375.
3. Moutaz A. Al-Dabbas and Hussain Zaydan Ali, "Geomorphological Mapping of Razzaza–Habbaria Area using Remote Sensing Techniques," Baghdad Science Journal, 13(1), pp. 155-166, 2016. https://doi.org/10.21123/bsj.2016.13.1.0155.
4. Taghreed Abdulhameed Naji, Shahad Abdul-Qader Abdul-Hameed, Dahlia Abdul-Qader Abdul-Hameed, Tabarak Mohammed Awad, and Sura Sabah Rasool Fakhruldeen "The use of remote sensing technology in defining the water depth in the lakes and water bodies: Western Iraq as a case study", J. Glob. Innov. Agric. Sci, 11(2):191-197, 2023. DOI: 10.22194/JGIAS/11.1083.
5. Bartłomiej Szypuła, "Quality assessment of DEM derived from topographic maps for geomorphometric purposes," Open Geosciences, vol. 11, pp. 843-865, 2019. DOI: 10.1515/geo-2019-0066.
6. W Zhang and D Montgomery, "Digital elevation model grid size, landscape representation, and hydrologic simulations," Water Resources Research, vol. 30, no. 4, pp. 1019–1028, 1994. https://doi.org/10.1029/93WR03553.
7. Aya Mohammed Hapep and Maythm AL-Bakri, "Comparison of Different DEM Generation Methods based on Open Source Datasets," Journal of Engineering, vol. 26, no. 1, pp. 63-85, 2020. https://doi.org/10.31026/j.eng.2020.01.07.
8. Ali Abdul-Jaleel Hussain and Muaid Jassim Rasheed, "Analysis of Morphological Features of Sargalu Region in Sulaymaniyah Governorate, North of Iraq, by using Geographic Information System," *Iraqi Journal of Science*, vol. 62, no. 4, pp. 1164-1176, 2021. https://doi.org/10.24996/ijs.2021.62.4.13.
9. Mushtaq Majed, and Hameed Majeed Abduljabbar, "The Change in the Land Cover of Mahmudiyah City in Iraq for the Last Three Decades", *Ibn AL-Haitham Journal For Pure and Applied Sciences*, 35(3), 44-55, 2022. https://doi.org/10.30526/35.3.2831.

10. METI/ERSDAC, NASA/LPDAAC, and USGS/EROS, "ASTER Global DEM Validation Summary Report," ASTER GDEM, 2009.
11. Evelyn Uuemaa, Sander Ahi , Bruno Montibeller, and Merle Muru, "Vertical Accuracy of Freely Available Global Digital Elevation Models (ASTER, AW3D30, MERIT, TanDEM-X, SRTM, and NASADEM," *Remote Sensing*, 12(21), pp. 1-23, 2020. https://doi.org/10.3390/rs12213482.
12. Alaa N. Hamdon, Laith kh. Ibraheem, and Ghazi A. Hussain, "Study of the Rocks and Analysis of Morphotectonic Uplift Between Kirkuk and Qara Chauq Anticlines Using Remote Sensing Techniques," *Iraqi Journal of Science*, 61(7), pp. 1684-1690, 2020. https://doi.org/10.24996/ijs.2020.61.7.17.
13. Taghreed Abdulhameed Naji, and Amal J. Hatem, "New adaptive satellite image classification technique for al Habbinya region west of Iraq", *Ibn AL-Haitham Journal For Pure and Applied Science*, 26(2), 143-149, (2013).
14. Michael Abrams, Robert Crippen, and Hiroyuki Fujisada, "ASTER Global Digital Elevation Model (GDEM) and ASTER Global Water Body Dataset (ASTWBD)," *Remote Sensing*, 12(7), pp. 1-12, 2020. https://doi.org/10.3390/rs12071156.
15. Aqeel A. Abdulhassan, Ahmed A. Naji, and Haqi H. Abbood, "Vertical Accuracy of Digital Elevation Models Based on Differential Global Positioning System," *Iraqi Journal of Science*, vol. Special Issue2, pp. 91-99, 2021. https://doi.org/10.24996/ijs.2021.SI.2.10.
16. Nehad Hameed and Taghreed Abdulhameed Naji, "Assessing Landsat Processing Levels and Support Vector Machine Classification", *Ibn AL-Haitham Journal For Pure and Applied Sciences*, 38(1), 197-209, 2025. https://orcid.org/0009-0005-9604-3324.
17. Muna Aref Mohammed, and Amal Jabbar Hatem, "Change detection of the land cover for three decades using remote sensing data and geographic information system*", AIP Conference Proceedings,* 2307 (1), 2020. https://doi.org/10.1063/5.0033261.
18. R Lyons Thomas, "REMOTE SENSING A Handbook for Archeologists and Cultural Resource Managers," Washington, D.C., 1977.
19. Minakshi Kumar and Ashutosh Bhardwaj, "Building Extraction from Very High Resolution Stereo Satellite Images Using OBIA and Topographic Information," *Environ. Sci.* , 5(1), pp. 1-6, 2021. https://doi.org/10.3390/IECG2020-08908.
20. Shangmin Zhao, Danning Qi, Rongping Li, Weiming Cheng, and Chenghu Zhou, "Performance comparison among typical open global DEM datasets in the Fenhe River Basin of China," *EUROPEAN JOURNAL OF REMOTE SENSING*, 54(1), pp. 145-157, 2021. https://doi.org/10.1080/22797254.2021.1891577.
21. Michael Abrams and Robert Crippen, "ASTER GDEM V3 (ASTER Global DEM)," U.S., 2019.
22. Guosong Zhao, Huaiping Xue, and Feng Ling, "Assessment of ASTER GDEM performance by comparing with SRTM and ICESat/GLAS data in Central China," , Wuhan, China, 2010. DOI: 10.1109/GEOINFORMATICS.2010.5567970.
23. K. Jacobsen and R. Passini, "ANALSYSIS OF ASTER GDEM ELEVATION MODELS," , USA, 2010.
24. Bernadett Dobre, István P. Kovács, and Titusz Bugya, "Comparison of digital elevation models through the analysis of geomorphic surface remnants in the Desatoya Mountains, Nevada," Hungary, 2021. https://doi.org/10.1111/tgis.1281.
25. ERSDAC and NASA's. (2020) Land Processes Distributed Active Archive Center (LP DAAC). [Online]. http://www.gdem.aster.ersdac.or.jp.
26. United State Geological Survey. (1987) EarthExplorer-Home. [Online]. http://earthexplorer.USGS.gov.
27. Shahad Abdul-Qader Abdul-Hameeda, and Amal Jabbar Hatem, "The Effect of Tidal Energies on the Materials Properties of the Soil", *Materials Science Forum*, 1050, 163-172, 2022. https://doi.org/10.4028/www.scientific.net/MSF.1050.163.
28. Yasser Yassin Khudair, Taghreed Abdulhameed Naji, Tabarak Mohammed Awad, Riyam Abd Al-Zahra Fadil, Shahad Abdul-Qader Abdul-Hameed, and Abdulrahman Bilal Ali, "Classification of East Shatt al-Arab Using the Novel Scene Optimum Index Factor (SOIF) and Spectral Angle Mapper classifier," *Journal of Physics: Conference Series*, 3028, (2025) 012056, 2025. doi:10.1088/1742-6596/3028/1/012056.
29. Ministry of Water Resources, General Authority for Groundwater, Geological Maps, Baghdad. 2018.

30. Zainab Q Al-Mudhafar and Sa'ad Z Al-Mashaikie, "Petrology and Mineralogy of Jabal Sanam Carbonate Rocks, Basrah, Iraq," *Journal of University of Babylon for Pure and Applied Sciences*, vol. 27, no. 3, pp. 130-142, 2019.
31. V K Sissakian, N Al-Ansari, and S Knutsson, "Geomorphology, Geology and Tectonics of Jabal Sanam, Southern Iraq," *Journal of Earth Sciences and Geotechnical Engineering*, 7(3), pp. 97-113, 2017.
32. R W Fairbridge, *The Encyclopedia of Geomorphology*, 1st ed. New York: Reinhold, 1968.
33. B Soltan, A Al-Fregi, and Z A Abdulnabi, "Petrogenesis of sedimentary ironstones in jabal sanam structure southern Iraq," *MARINA MESOPOTAMICA*, 22(1), pp. 93-105, 2007.
34. Taghreed Abdulhameed Naji, Ali Adnan N. Al-Jasim, Auday H. Shaban, and Hameed Majed Abduljabbar, "Spatial Analyzing of the Chemical Soil Properties for the Sanam Mountain- Al Zubair Region South of Basra Province and Diagnosis of its Effects on Soil Qualities Using Remote Sensing Technology and GIS," *Materials Science Forum*, 1050, 173-187, 2022. https://doi.org/10.4028/www.scientific.net/MSF.1050.173.
35. Shahad Abdul-Qader Abdul-Hameed, and Amal Jabbar Hatem, “Effect of Shatt Al-Arab salinity on the groundwater of Al-Fao and Al-Siba in Southern Iraq”, *Iraqi Geological Journal*, 54 (1E), 114-122, 2021. https://doi.org/10.46717/igj.54.1E.10Ms-2021-05-31.